Direct Arylation Polymerization of Degradable Imine-based Conjugated Polymers

Nathan Sung Yuan Hsu[1], Angela Lin[1], Azalea Uva[1], Shine Han Huang[1], Helen Tran[1,2,3]*

[1]Department of Chemistry, University of Toronto, 80 St. George Street, Toronto, ON M5S 3H6, Canada

[2]Department of Chemical Engineering and Applied Chemistry, University of Toronto, 200 College St, Toronto, ON M5S 3E5, Canada

[3]Acceleration Consortium, University of Toronto. 80 St George St, Toronto, ON M5S 3H6

Keywords: Green synthesis, imine-based polymers, degradable polymers, direct arylation polymerization, indacenodithiophene

ABSTRACT: The development and optimization of reliable polymerization methods are needed for the synthesis of degradable imine-based conjugated polymers, which are attractive materials for transient electronics. Direct arylation polymerization (DArP) has emerged as a sustainable and atom-economical synthetic method for the preparation of well-defined conjugated polymers. Compared to polymerization methods such as imine polycondensation or Stille cross-coupling polymerization which require monomer functionalization, direct arylation proceeds via C-H activation and thereby reduces synthetic complexities and toxic by-products. Here we report the first use of DArP for the synthesis of an imine-based indacenodithiophene (IDT) copolymer, p(IDT-TIT). Polymers prepared via DArP can result in branched or cross-linked polymer chains due to the reactivity of C-H bonds in the monomers. In this report, we demonstrate a systematic study focusing on the reaction conditions needed to prepare p(IDT-TIT) via DArP with tetramethylethylenediamine as a co-ligand. The degradable polymer is characterized via nuclear magnetic resonance spectroscopy, high-temperature gel permeation chromatography, and ultraviolet-visible-near-infrared spectroscopy. With the simplicity of monomer preparation and reaction conditions, we anticipate this efficient synthetic protocol will lead to higher synthetic adoption in the research community to aid the exploration of high-performance imine-based degradable materials.

Introduction. Conjugated polymers form the pillar of many new technological advances owing to their vast design space that harmonizes the optical and electronic properties of inorganic materials with simple solution processing and potential lower cost offered by polymers. Using conjugated polymers for the next generation of electronic devices has attracted significant research attention due to distinct advantages such as stretchability, mechanical flexibility, and biocompatibility that can be achieved through tunable structure-functional relationships. These properties have been leveraged in applications such as in organic photovoltaics,[1,2] biological sensing and metabolite monitoring,[3,4] drug delivery and therapeutics,[5–7] photothermal therapy, [8,9] and bioelectronics.[10–12] However, the aspect of degradability has not been explored to the same extent.[13,14] We anticipate that such electronics will seemingly integrate with our lives in the future; thus, efforts endowing conjugated polymers with transience via controlled degradation is needed to enable the development of advanced

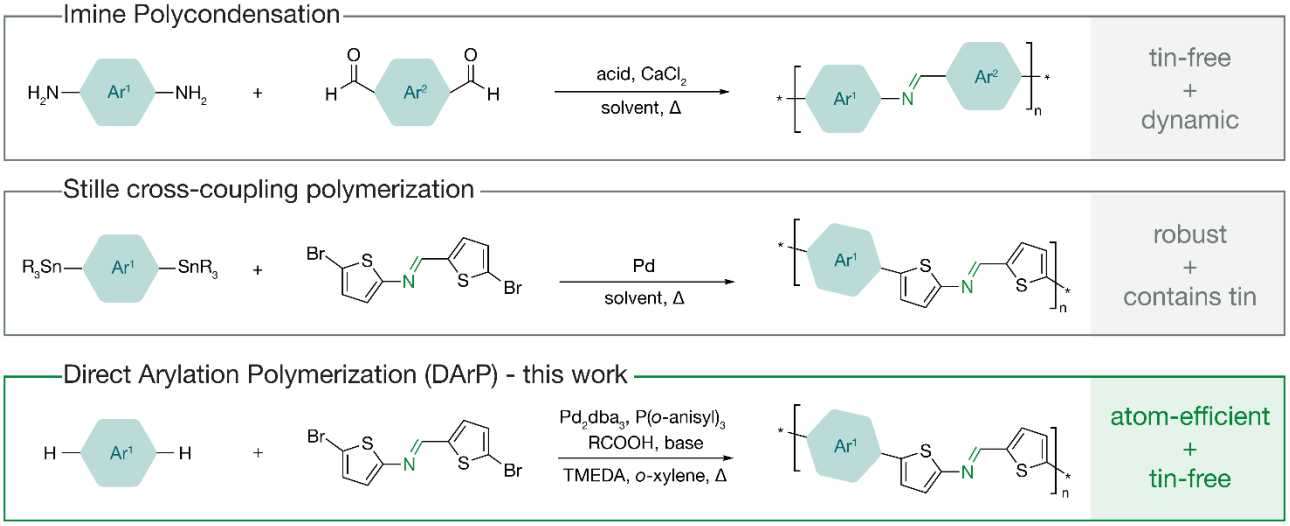

Figure 1. Polymerization approaches towards synthesizing degradable imine-based conjugated polymers. Expanding the synthetic toolbox to assess degradable imine-based conjugated polymers by direct arylation polymerization provides an atom-efficient and greener alternative to overcome the limitations of current imine polycondensation and Stille cross-coupling polymerization methods.

healthcare devices, and preemptively alleviate electronic waste concerns.[15–20]

An attractive strategy to impart transience to conjugated polymer is incorporating linkages that are susceptible to hydrolysis or oxidation along the polymer backbone. This allows for the complete chemical breakdown of conjugated polymers that can be triggered once the device reaches its end-of-life fate.[21] Through judicious monomer and polymer designs, degradation can occur from an external stimulus, such as a specific change in physiological conditions, allowing for fine tuning of degradation lifetimes.[17] In some instances, degradation can also lead to the recovery of the starting monomers, establishing a circular closed-end loop through recyclability.[22,23] Although these linkages have been investigated, they often compromise electrical performance. Recent work has demonstrated that conjugated polymers containing imine bonds can be readily degraded via acid hydrolysis while maintaining electronic performance comparable to their non-degradable vinyl counterpart.[24,25] Moreover, the tunable optoelectronic properties of imine-based conjugated polymers have also been extensively investigated by Skene and coworkers.[26–28] The scope of imine-based conjugated polymers established by these earlier reports has since motivated new monomer and polymer designs. For example, Bao and coworkers designed thiophene-imine-thiophene (TIT), which through copolymerization with diketopyrrolopyrrole (DPP) and naphthalene diimide (NDI), yielded two new degradable polymers.[29] Since then, Bao and coworkers have explored the tunability of degradation lifetimes of TIT-based conjugated polymers.[30] Collier and coworkers leveraged the diverse properties and synthetic versatility of the dihydropyrrolo[3,2-b]pyrrole monomeric scaffold to synthesize a new degradable polymer furnished with imine bonds.[23] Work from our group demonstrated that biobased monomers from carotenoids can give rise to imine-based, carotenoid-phenylenediamine polymers, which resemble the structure of polyacetylene.[31] The emergence of new polymers relies on robust and efficient polymerization methods to afford well-defined polymers. To date, degradable imine-based conjugated polymers are mainly synthesized via imine polycondensation or Stille cross-coupling polymerization (Figure 1). Imine polycondensation involves diamine and dialdehyde monomers, which may require additional synthetic steps in their preparation.[31] On the other hand, Stille cross-coupling polymerization has proven to be a robust and versatile method since the synthetic toolbox to assess aryl halides and stannylated reagents is more established than functionalizing aryl monomers with imines and aldehydes.[29] However, Stille cross-coupling polymerizations have poor atom efficiency, and their synthesis and purification involves toxic stannylated reagents and produces stoichiometric organotin waste. These caveats hinder the feasibility of their large scale-up. As the investigation of degradable imine-based conjugated polymers advances, the synthetic toolbox to synthesize them will need to expand to include atom-efficient and benign polymerization methods with direct arylation polymerization (DArP) being a prime candidate.[32–34] DArP circumvents the requirements to pre-functionalize a coupling partner with a sacrificial organometallic moiety, enabling the desired polymer to be synthesized with fewer synthetic steps.

Herein, we demonstrate the synthesis of a new imine-based copolymer, in which indacenodithiophene (IDT) is copolymerized with dibrominated TIT via DArP. IDT has gained popularity as a building block for conjugated polymer due to its high charge carrier mobilities (> 1 $cm^2V^{-1}s^{-1}$) and stretchability when copolymerized with benzothiadiazole (BT), to form p(IDT-BT).[35–38] By copolymerizing with dibrominated TIT instead of dibrominated BT, we prepared p(IDT-TIT) by DArP, the first example of a degradable IDT-based copolymer to the best of our knowledge (Figure 1). In addition, this work is the first to prepare imine-based conjugated polymers by DArP, where p(IDT-TIT) with isolated

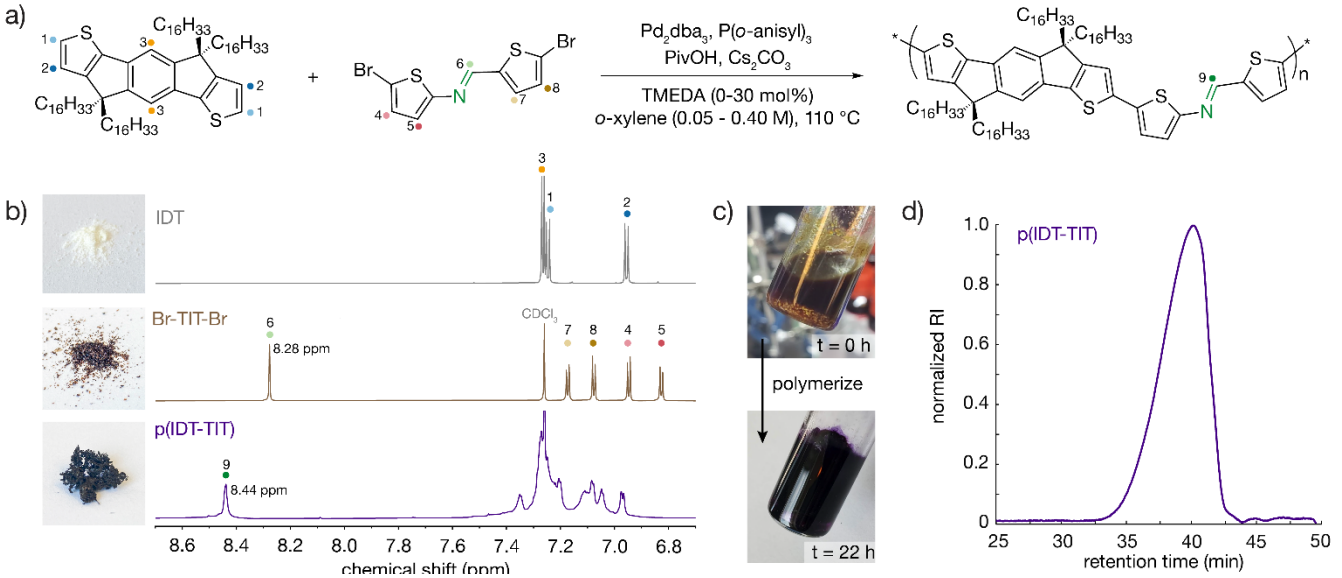

Figure 2. The synthesis of degradable imine-based conjugated polymer p(IDT-TIT) by direct arylation polymerization (DArP) (a) General DArP conditions explored to synthesize p(IDT-TIT). (b) ^{1}H NMR spectra of the starting materials IDT and Br-TIT-Br compared to the p(IDT-TIT) with a distinct downfield shift of the imine proton from 8.28 to 8.44 ppm. (c) Photographs of the polymerization between IDT and Br-TIT-Br, forming p(IDT-TIT) after 22 hours accompanied by a distinct color change from yellowish-brown to purple. (d) HT-GPC chromatogram of p(IDT-TIT) from Table 1 entry 10 showing a unimodal peak.

with M_n of 12 kg/mol in the hexane fraction and 25 kg/mol in the chlorobenzene fraction. p(IDT-TIT) was characterized by ^{1}H nuclear magnetic resonance and high-temperature gel permeation chromatography (HT-GPC), and its acid degradation properties were characterized by ultraviolet-visible-near-infrared (UV-vis-NIR) absorption spectroscopy. Establishing the use of DArP as an alternative synthetic route to assess degradable imine-based conjugated polymers will encourage exploration of future degradable polymers via a more sustainable method.

Synthesis and Polymerizations. p(IDT-TIT) was synthesized via DArP between IDT and dibrominated TIT (Br-TIT-Br) (Figure 2a). Detailed synthetic protocols and characterization of the polymer and monomer can be found in the Supporting Information (SI, monomer: Figure S1-S7, polymer: Figure S8-S10). The successful use of DArP as an alternative polymerization method to synthesize IDT-copolymers between IDT as the C-H monomer and dibrominated comonomers such as BT, NDI, thiapyrollodione (TPD), and benzopyrroledione (BPD), have been explored in recent literature.[37,41–43] Inspired by the success of Ozawa's DArP conditions between IDT with other brominated comonomers, we initially tried to synthesize p(IDT-TIT) utilizing Pd_2dba_3, P(*o*-anisyl)$_3$ with *o*-xylenes (Table 1). Although a color change from dark amber to dark red was observed during our preliminary polymerization, a minimal amount of solid precipitate was collected when the crude was precipitated in methanol (MeOH, Table 1, entry 1). Due to the low yield, only high-temperature gel permeation chromatography (HT-GPC) characterization was performed, and the M_n was determined to be 3.1 kg/mol. These initial results were unsurprising, because of earlier unsuccessful attempts by Wang and coworkers at using DArP to synthesize a conjugated polymer consisting of thiophene-vinyl-thiophene (TVT), an isoelectronic analog of TIT.[44] Instead, Wang and coworkers studied a fluorinated TVT derivative in which all β- and γ- C-H positions were fluorinated, which led to polymers with high M_n (60 kg/mol) via DArP. Given our results and these previous literature findings, we hypothesize that non-selective C-H activation at the β- and γ- positions of TIT could be occurring, resulting in branching defects that would explain the low M_n and yield observed with our p(IDT-TIT) system. The adverse effects of undesired cross-coupling (i.e. branching, homocoupling) associated with DArP, albeit often to a small extent, lead to significant hindrance in desired optoelectronic properties.[32,45] The prevention and evaluation of these defects are a major limitation with DArP as it often occurs in small quantities, specific to the monomers system being studied, and poses a challenge to identify.

Table 1. Optimization of Direct Arylation Polymerization (DArP) for p(IDT-TIT).[a]

Entry	TMEDA[a] (mol%)	[IDT] (M)	Yield[a] (%)	M_n[b] (kg/mol)	Đ[b]
1	0	0.05	N/A[c]	3.1[c]	2.30[c]
2	5	0.05	N/A[c]	5.8[c]	1.24[c]
3	10	0.05	28	13.6	1.97
4	15	0.05	45	12.5	1.94
5	30	0.05	13	10.7	1.72
6	10	0.09	23	13.6	1.88
7	10	0.40	10	11.2	1.67
8[d]	10	0.40	20	12.6	1.66
9	0	0.40	10	12.4	1.55
10[d]	10	0.25	26	12.7	1.84

[a]DArP reaction conditions unless otherwise noted: 1:1 stoichiometric ratio between IDT and Br-TIT-Br. Pd_2dba_3 5 mol%, P(*o*-anisyl)$_3$ 10 mol%, Cs_2CO_3 3.0 equiv., PivOH 1.0 equiv., with TMEDA as listed, [IDT] concentration as listed at 110 °C for 22 h in anhydrous *o*-xylenes. Yields are isolated yields collected in the hexane fraction via Soxhlet extraction. [b]Determined by HT-GPC at 135 °C in 1,2,4-trichlorobenzene. [c]Crude yield < 1% and cannot be isolated for weighing. [d]1:1 stoichiometric ratio between IDT (200 mg) and Br-TIT-Br scale polymerization. [e]1:1 stoichiometric ratio between IDT and Br-TIT-Br, Pd_2dba_3 2 mol%, P(*o*-anisyl)$_3$ 8 mol%, Cs_2CO_3 3.0 equiv., PivOH 1.0 equiv., at 100 °C for 22 h in anhydrous *o*-xylenes.

To increase M_n and yields, pioneering work from Ozawa and coworkers have identified that adding tetramethylethylenediamine (TMEDA) as a co-ligand in DArP minimized cross-coupling defects in their copolymer system consisting of dithienosilole (DTS) and TPD.[46] This mixed-ligand approach, which combines the use of TMEDA and P(*o*-anisyl)$_3$, has since successfully achieved high M_n (> 20 kg/mol) and yields (> 80%) in polymer systems that are historically plagued with structural defects like DPP, benzodithiophene (BDT), and other monomers despite their abundance of potential C-H activation sites.[46–48] Inspired by these results, we attempted to synthesize p(IDT-TIT) by adding various stoichiometric amounts of TMEDA (0 to 30 mol%) as a co-ligand (Table 1). For 10-30 mol% TMEDA, a distinct color change was observed upon polymerization from dark amber to dark purple (Table 1, entries 3-5, Figure 2c). In addition, the crude yield was isolated when precipitated in MeOH. This contrasted with the minimal solids obtained for polymerization without TMEDA. The crude solids were purified via Soxhlet extraction with most of the mass recovered in the hexane fraction corresponding to the desired p(IDT-TIT) product as characterized by ^{1}H NMR spectroscopy and HT-GPC. By ^{1}H NMR spectroscopy, successful polymerization was confirmed with the downfield shift of the signal corresponding to the imine N-H proton from 8.28 ppm in Br-TIT-Br to 8.44 ppm in p(IDT-TIT) (Figure 2b, Figure S9). Although 15 mol% TMEDA resulted in a higher yield than 10 mol% (45.1% compared to 27.8%), its M_n was lower. Interestingly, 5 mol% TMEDA was insufficient at affording the p(IDT-TIT) polymer with an isolated yield and HT-GPC data showed only a minor improvement in M_n compared to catalytic conditions without TMEDA (Table 1, entry 2). At 30 mol% TMEDA, the M_n was 10.7 kg/mol, lower than the 13.6 kg/mol observed for 10 mol% TMEDA. Based on these results, 10 mol% TMEDA afforded p(IDT-TIT) with the highest M_n.

Since 10 mol% TMEDA resulted in the highest M_n amongst the different TMEDA concentrations studied, increasing the monomer concentration with respect to IDT was an additional parameter varied to obtain higher M_n. Previous studies have investigated the effects of M_n as a function of monomer concentration and observed that high monomer concentration led to higher M_n.[49–51] These results corroborate with kinetic experiments performed by Fagnou and coworkers, concluding the first-order dependency of the C-H monomer concentration in the direct arylation mechanism.[52] For our p(IDT-TIT) system, a slight increase

in crude (i.e. before Soxhlet) M_n from 13.9 kg/mol to 15.2 kg/mol when the monomer concentration increased from 0.05 M to 0.09 M, respectively; however, the M_n isolated from the hexane fraction remained similar (Table 1, entry 3 and 6). We believe this was due to the lack of solubility of the higher M_n polymers in the crude to be soluble in hexanes. Further increase in monomer concentration to 0.40 M resulted in a slightly lower M_n of 11.2 kg/mol with a low yield of 10% (Table 1, entry 7). The lower M_n and yield could be due to the extremely low volume of solvent in the vial to meet the 0.40 M concentration at a 40 mg scale, such that stirring and covering all solid reagents in the vial was difficult. To eliminate this factor, a 200 mg scale polymerization at 0.40 M concentration was conducted to ensure all reagents could be dissolved and suspended to maintain consistent stirring. Interestingly, only a slight difference in M_n was noticed between the 40 mg scale and the 200 mg scale 0.40 M concentration batches (Table 1, entry 7 and 8). We also conducted a negative control by polymerizing without TMEDA at 0.40 M concentration (Table 1, entry 9). This would help delineate whether it is the addition of TMEDA and/or the increase in monomer concentration from 0.05 M to 0.40 M that enabled successful polymerization. To our surprise, at the higher monomer concentration of 0.40 M, a M_n of 12,600 g/mol was achieved without adding TMEDA, which is comparable to the M_n achieved with 10 mol% TMEDA. Thus, at 0.40 M concentration, successful polymerization was achieved with or without TMEDA, which contrasts with the results observed at 0.05 M concentration, in which TMEDA was needed for polymerization to occur. Although similar M_n was achieved for the 0.40 M concentration with and without TMEDA, there were noticeable differences when comparing their ^{1}H NMR spectra, as the polymerization without TMEDA had additional signals that suggest the presence of structural defects (Figure S11). To address issues with solvation during polymerization, 10 mol% TMEDA at 0.25 M concentration was conducted (Table 1, entry 10). Although higher monomer concentration is favorable for DArP to achieve higher M_n, at a certain concentration, unwanted precipitation of the polymer from the reaction medium occurs, limiting the formation of polymers with higher M_n.[49,51,53] This was also supported by the gelation observed when polymerizing p(IDT-TIT) on the 40 mg and 200 mg scale at 0.40 M concentrations (Figure S12). The M_n for the 0.25 M concentration of 12.7 kg/mol was similar with that of 0.40 M, even though the polymerization itself did not reach gelation but was viscous (Figure 2d).

Upon further investigation, we noticed significant amounts of purple solids that remained in the glass thimble at both the 0.25 M and 0.40 M concentrations that were partially soluble in hot chlorobenzene (Figure S13). HT-GPC characterization of these solution showed M_n of 25.3 and 25.2 kg/mol for 0.25 M and 0.40 M concentrations, respectively (Figure S14). These results indicate that synthesizing p(IDT-TIT) to higher M_n could be limited due to its solubility. Our attempts to polymerize with a microwave synthesizer at 160 °C for 40 mins rather than the conventional approach of using a hotplate in the glovebox did not yield any polymeric product (Figure S15). Overall, our attempts to synthesize p(IDT-TIT) by adapting existing protocols highlight the sensitivity of DArP to specific comonomer systems. Based on the polymerization conditions tried, the DArP parameters consisting of Pd_2dba_3, P(*o*-anisyl)$_3$, Cs_2CO_3, and pivalic acid with 10 mol% TMEDA in *o*-xylenes (0.25 M) at 110 °C for 22 hours was determined to be optimal for the synthesis of p(IDT-TIT) for our studies. Thus, all characterization henceforth was from this trial (Table 1, entry 10, Figure S8-S9).

Solution Photophysical Properties and Degradation Studies. The degradation of imine-conjugated polymers by acid hydrolysis is typically investigated to study their degradation profile and lifetimes.[22,24,31,54] The degradation of the imine bonds were investigated by treating p(IDT-TIT) with various % v/v trifluoracetic acid (TFA) and monitored with UV-vis-NIR spectroscopy. The resulting absorbance shifts are summarized in Table 2.

The effect of acid concentration on the rate of hydrolysis was studied by designing a concentration-dependent degradation investigation. Solutions of p(IDT-TIT) (chlorobenzene, 0.01 mg/mL) treated with 0 to 2% v/v TFA concentration were monitored by UV-vis-NIR spectroscopy with the hypothesis that higher TFA concentration will result in a hypochromic shift of the spectra as shorter oligomers are formed (Figure 3c).[24,25] The maximum absorbance wavelength (λ_{max}) of p(IDT-TIT) was 570 nm, ascribed to its charge transfer (CT) band. The λ_{max} is comparable to other IDT-copolymer systems.[37] Interestingly, instead of hypochromic shift, a large bathochromic shift of approximately 208 nm was observed from the p(IDT-TIT) with no TFA to the 2% v/v TFA. We hypothesize that the bathochromic shift, forming a lower energy peak at 778 nm, corresponds to the protonated quinoidal structure of the polymer due to the increased electron deficiency when the nitrogen of the imine is protonated.[55] It has been previously demonstrated that imine bonds can undergo protonic acid-doping, in which the imine bond is protonated, favoring the formation of a proposed quinoidal structure of the polymer with exocyclic double bonds (Figure 3a).[56,57] Polymers that favor the quinoidal structure have been investigated for their application in *n*-type thermoelectric devices and *n*-type organic transistors as they exhibit a profound narrowing of the HOMO-LUMO bandgap and exhibit lower-lying LUMO compared to their benzenoidal counterparts.[58–61] Although 2% v/v TFA showed a prominent shift, the presence of this lower energy absorbance peak begins to emerge at 0.03% v/v TFA. At 0.09% v/v TFA, the original p(IDT-TIT) peak at 570 nm was accompanied by approximately an equal intensity peak at 725 nm. The λ_{max} of the lower energy peak shifted from 725 nm to 778 nm as its intensity increased to become the main peak as the % v/v TFA changed from 0.09% to 2%. We hypothesize that as higher TFA concentration was added, the equilibrium between the undoped benzenoidal structure shifts favorably to the doped quinoidal structure, in which exocyclic double bonds are formed between TIT and IDT, rigidifying the polymer backbone and narrowing the bandgap.[56–61] An isosbestic point was observed at *ca.* 640 nm, which corroborated the presence of only two species – the undoped and doped species, a feature observed in other imine-based conjugated polymers.[62] The bathochromic shift in the UV-Vis spectra was also accompanied by a color change from purple to blue as TFA was added, supporting the proposed doped quinoidal structure (Figure 3b). Overall, these observations were consistent

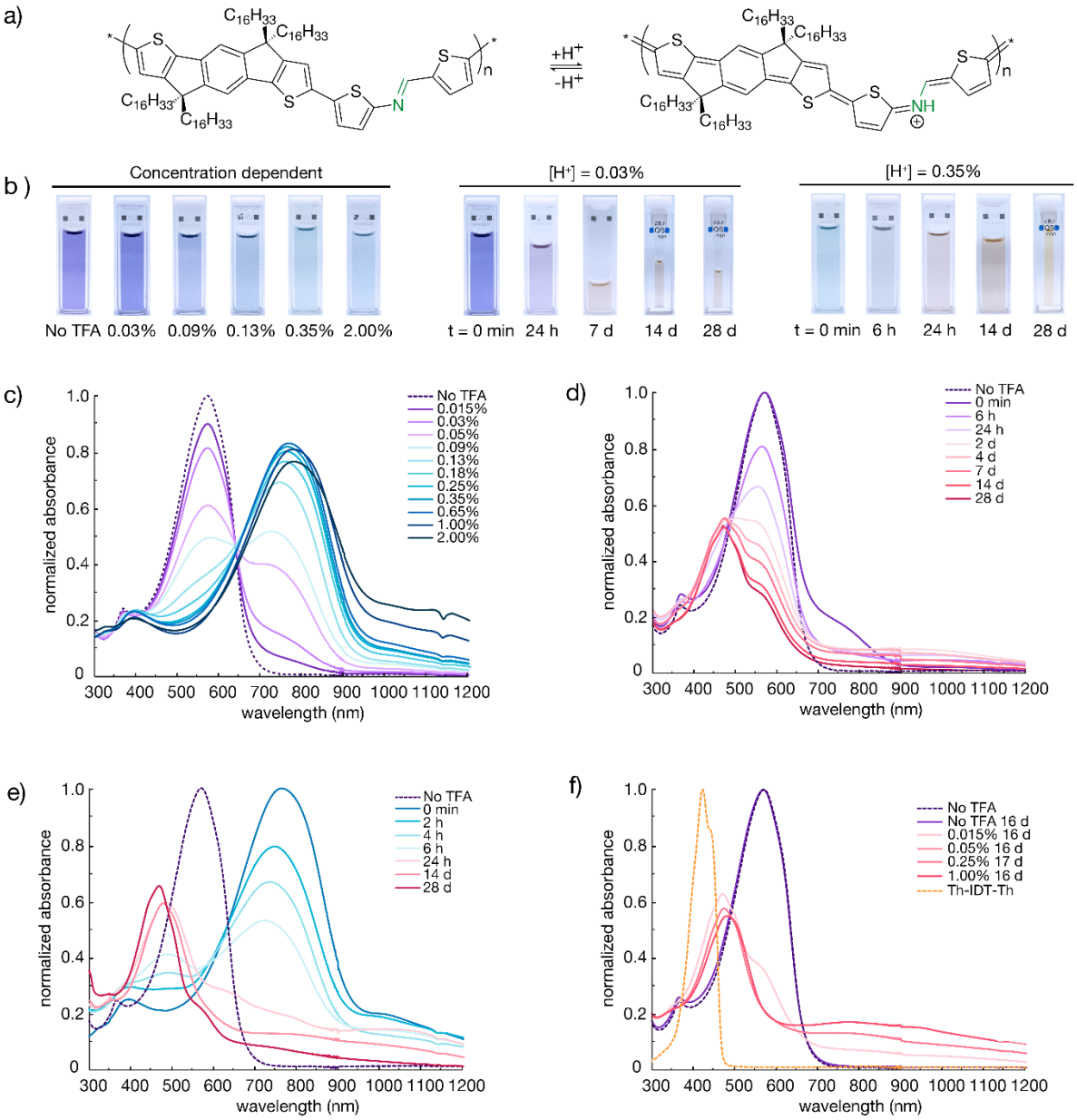

Figure 3. Degradation studies of p(IDT-TIT) with various % v/v TFA in chlorobenzene by UV-vis-NIR spectroscopy. (a) Protonation of the imine-bond shifts the equilibrium to favor the proposed protonated quinoidal structure (right) over the benzenoidal-structure (left), leading to a bathochromic shift of λ_{max}. (b) Photographs of p(IDT-TIT) solution treated with 0-2% v/v TFA and at stated time points during the degradation study with low TFA (0.03% v/v) and high TFA (0.35% v/v). (c) Concentration-dependent degradation study with 0-2% v/v TFA. (d) Time-dependent degradation study with low TFA (0.03% v/v). (e) Time-dependent degradation study with high TFA (0.35% v/v). (f) Degradation of samples treated with various % v/v TFA after ca. two weeks with Th-IDT-Th as the degraded model compound.

with the protonation of other imine-based conjugated polymers documented in literature.[22,55,56,63]

The progression of degradation over time was investigated spectroscopically for samples treated with low (0.03%) and high (0.35%) v/v TFA (Figure 3d and 3e). Although a minor shoulder *ca.* 750 nm at 0 min was observed for 0.03% v/v TFA, its absorbance did not increase over time (Figure 3d). From 1 to 28 days, a shoulder of lower wavelength at 471 nm appeared and became more resolved as the absorbance of the original peak at 570 nm diminished. During this same period, the sample visibly turned from purple to light purple, then pale peach as p(IDT-TIT) degraded (Figure 3b). In contrast, for 0.35% v/v TFA at 0 min, there was an emergence of the lower energy peak at 762 nm as the polymer is doped to favor the quinoidal structure with a narrowed bandgap compared to the original p(IDT-TIT) peak at 570 nm (Figure 3e). As expected, the imine bonds are more readily hydrolyzed at a higher % v/v TFA as shown by a faster decrease in absorbance of the λ_{max} compared to what was observed for 0.03% v/v TFA. In addition, a hypochromic shift was observed from 762 nm to 722 nm after 6 hours, which we attribute to the formation of shorter oligomers as the polymer backbone in the

quinoidal structure is hydrolyzed. Similar to 0.03% v/v TFA, a lower wavelength peak, *ca*. 490 nm, appeared after 4 hours, then fully developed to one peak at 469 nm by 28 days, at which the peak associated with the doped quinoidal structure is no longer present. The color of p(IDT-TIT) treated with 0.35% v/v TFA and 0.03% TFA were comparable by 28 days (peach color), suggesting similar degradation products are formed (Figure 3b). This color change (purple to peach) was observed for all samples treated with varied % v/v TFA, which aligns with the appearance of an absorption peak in the range of 471-478 nm (Figure 3f).

Since all samples showed similar absorption traces after two weeks, we wanted to explore the possibility that p(IDT-TIT) hydrolyzed to form a new asymmetric IDT-based monomer, which we propose to be an IDT flanked with a thiophene-2-carboxaldehyde and a 2-aminothiophene (Figure S16). However, we were unable to decipher the matrix-assisted laser desorption/ionization time-of-flight (MALDI-ToF), direct analysis in real time (DART), and electrospray ionization (ESI) mass spectrometry of the degraded products. A similar symmetric IDT-based monomer with flanking thiophenes (Th-IDT-Th) was synthesized to help identify the degraded products that formed (Figure S16). However, the absorption spectrum of Th-IDT-Th with a λ_{max} of 422 nm, which did not align with the λ_{max} (471-478 nm) observed in the spectra from the degradation studies (Figure 3f). We recognize there is a difference between our predicted degraded product and the model Th-IDT-Th compound, which could be the reason for the difference in the λ_{max} observed. Further investigation to identify these degradation byproducts is merited.

Thin film studies and TFA vapor doping. Thin film investigations were conducted to understand the acid-doping properties of p(IDT-TIT) in solid-state compared to in solution. Thin film samples were spin-cast from a chlorobenzene solution of p(IDT-TIT) onto glass slides and their absorption spectra were acquired (Figure 4a). Without TFA, a minimal shift in the absorption spectra between thin film and in solution was noticed and is consistent with other IDT-based copolymers, which is attributed to the weak intermolecular interactions resulting from the -$C_{16}H_{33}$ alkyl chains of IDT.[37] Enclosed with a cuvette saturated with TFA vapor, p(IDT-TIT) thin film exhibited a bathochromic shift of 282 nm and a λ_{max} at 837 nm. Similar to in solution, a distinct color change from purple to light blue was observed for thin films treated with TFA vapor (Figure 4b). The pronounced spectroscopic and color changes in thin films and in solution as a result of protonic acid-doping suggest that p(IDT-TIT) displays sensor-like properties.[64,65]

Table 2. UV-vis-NIR spectroscopic data for concentration-dependent and time-dependent degradation studies of p(IDT-TIT) with TFA.[a]

	% v/v TFA	Time	λ_{max} (nm)
Concentration-dependent degradation	0	0 min	570
	0.015	0 min	570
	0.03	0 min	570
	0.05	0 min	570
	0.09	0 min	725
	0.13	0 min	743
	0.18	0 min	756
	0.25	0 min	759
	0.35	0 min	762
	0.65	0 min	765
	1.00	0 min	775
	2.00	0 min	778
Time-dependent degradation (low TFA concentration)	0.03	0 min	570
	0.03	6 h	564
	0.03	24 h	554
	0.03	2 d	507
	0.03	4 d	475
	0.03	7 d	473
	0.03	14 d	472
	0.03	28 d	472
Time-dependent degradation (high TFA concentration)	0.35	0 min	762
	0.35	2 h	748
	0.35	4 h	733
	0.35	6 h	722
	0.35	24 h	482
	0.35	14 d	476
	0.35	28 d	469

[a]Detailed procedures in setting these degradation studies can be found in the SI.

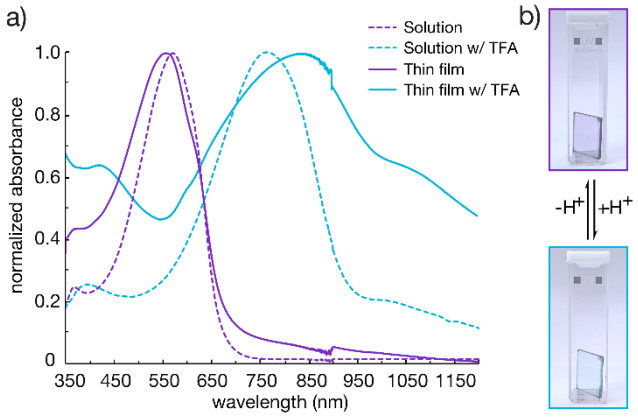

Figure 4. Thin film of p(IDT-TIT) spin-cast onto glass slides monitored by UV-vis-NIR spectroscopy. (a) Thin film of p(IDT-TIT) treated with neat TFA vapor showed a bathochromic shift of λ_{max} (purple solid to blue solid), compared to a representative solution treated with 0.35% v/v TFA (purple dotted to blue dotted). (b) Photographs of the thin films in a cuvette show a color change from purple to blue once treated with TFA vapor. Note: switchover at 900 nm resulted in an uneven stepwise transition in absorbance values for 900-1200 nm. This range was manually corrected when graphing data for thin film (purple solid).

Conclusion. In summary, we present DArP conditions to synthesize p(IDT-TIT), a degradable conjugated polymer. It was determined that TMEDA facilitates the successful polymerization of p(IDT-TIT) at low IDT concentration (0.05 M), whereas, in the absence of TMEDA, only short oligomers are formed with poor yields. However, at high IDT concentration (0.40 M), the addition or absence of TMEDA did not affect M_n, although yields were lower without TMEDA, and defects were observed by ^{1}H NMR spectroscopy. By synthesizing p(IDT-TIT), we demonstrated the versatility of utilizing DArP as a more environmentally sustainable, atom-efficient, and benign alternative to synthesize imine-based conjugated polymers, especially compared to

Stille cross-coupling polymerization. The imine bond incorporated within the structure of TIT confers p(IDT-TIT) with transient properties, which was investigated spectroscopically by concentration-dependent and time-dependent acid hydrolysis studies with TFA. p(IDT-TIT) undergoes protonic acid-doping dependent on acid concentration, resulting in a pronounced bathochromic shift of the CT band ascribed to the proposed quinoidal structure of the protonated p(IDT-TIT). At high acid concentration (i.e. 0.35% v/v TFA), p(IDT-TIT) degraded from the quinoidal structure; whereas at lower acid concentration (i.e. 0.03% v/v TFA), the polymer degraded from the benzenoidal structure. Either degradation pathways from the quinoidal or benzenoidal structures led to the formation of degraded products with λ_{max} *ca*. 470 nm. Our results help establish an alternative sustainable polymerization method to synthesize and investigate degradable imine-based conjugated polymers, encouraging future degradable conjugated polymers to be explored.

ASSOCIATED CONTENT

This material is available free of charge at http://pubs.acs.org. Detailed synthetic procedure, NMR, HT-GPC, and UV-Vis data available (PDF).

AUTHOR INFORMATION

Corresponding Author

*tran@utoronto.ca

Author Contributions

All authors have given approval to the final version of the manuscript. Conceptualization, methodologies, N.S.Y.H. and H.T.; monomer synthesis, N.S.Y.H. and S.H.H.; polymerization optimization, N.S.Y.H. and A.L.; data curation, N.S.Y.H and A.U.; data visualization and figure making, N.S.Y.H., A.U., A.L., and H.T.; writing–original draft N.S.Y.H., A.L., and H.T.; writing–reviewing/editing, all authors.

ACKNOWLEDGMENT

This work was supported by the Natural Sciences and Engineering Research Council (NSERC) of Canada (H.T., RGPIN2021-03554; A.L. and A.U., CGS-D scholarships), the Canadian Foundation for Innovation (H.T.: JELF-41743), and the Ministry of Colleges and Universities (N.S.Y.H., Ontario Graduate Scholarship) for funding this work. This research was undertaken thanks in part to funding provided to the University of Toronto's Acceleration Consortium from the Canada First Research Excellence Fund. The authors acknowledge the Department of Chemistry at the University of Toronto for their support.

REFERENCES

(1) Holliday, S.; Li, Y.; Luscombe, C. K. Recent Advances in High Performance Donor-Acceptor Polymers for Organic Photovoltaics. *Prog. Polym. Sci.* **2017**, *70*, 34–51. https://doi.org/10.1016/J.PROGPOLYMSCI.2017.03.003.

(2) Zhang, Z. G.; Li, Y. Polymerized Small-Molecule Acceptors for High-Performance All-Polymer Solar Cells. *Angew. Chem. Int. Ed.* **2021**, *60* (9), 4422–4433. https://doi.org/10.1002/ANIE.202009666.

(3) Lin, P.; Yan, F.; Lin, P.; Yan, F. Organic Thin-Film Transistors for Chemical and Biological Sensing. *Adv. Mater.* **2012**, *24* (1), 34–51. https://doi.org/10.1002/ADMA.201103334.

(4) Pappa, A. M.; Parlak, O.; Scheiblin, G.; Mailley, P.; Salleo, A.; Owens, R. M. Organic Electronics for Point-of-Care Metabolite Monitoring. *Trends Biotechnol.* **2018**, *36* (1), 45–59. https://doi.org/10.1016/j.tibtech.2017.10.022.

(5) Jonsson, A.; Song, Z.; Nilsson, D.; Meyerson, B. A.; Simon, D. T.; Linderoth, B.; Berggren, M. Therapy Using Implanted Organic Bioelectronics. *Sci. Adv.* **2015**, *1*, *e150003*. https://doi.org/10.1126/SCIADV.1500039.

(6) Liu, H.; Wang, K.; Yang, C.; Huang, S.; Wang, M. Multifunctional Polymeric Micelles Loaded with Doxorubicin and Poly(Dithienyl-Diketopyrrolopyrrole) for near-Infrared Light-Controlled Chemo-Phototherapy of Cancer Cells. *Colloids Surf., B* **2017**, *157*, 398–406. https://doi.org/10.1016/J.COLSURFB.2017.05.080.

(7) Yang, C.; Huang, S.; Wang, X.; Wang, M. Theranostic Unimolecular Micelles of Highly Fluorescent Conjugated Polymer Bottlebrushes for Far Red/near Infrared Bioimaging and Efficient Anticancer Drug Delivery. *Polym. Chem.* **2016**, *7* (48), 7455–7468. https://doi.org/10.1039/C6PY01838F.

(8) Yang, Y.; Fan, X.; Li, L.; Yang, Y.; Nuernisha, A.; Xue, D.; He, C.; Qian, J.; Hu, Q.; Chen, H.; Liu, J.; Huang, W. Semiconducting Polymer Nanoparticles as Theranostic System for Near-Infrared-II Fluorescence Imaging and Photothermal Therapy under Safe Laser Fluence. *ACS Nano* **2020**, *14* (2), 2509–2521. https://doi.org/10.1021/ACSNANO.0C00043.

(9) Chen, P.; Ma, Y.; Zheng, Z.; Wu, C.; Wang, Y.; Liang, G. Facile Syntheses of Conjugated Polymers for Photothermal Tumour Therapy. *Nat. Commun.* **2019**, *10* (1), 1–10. https://doi.org/10.1038/s41467-019-09226-6.

(10) Balakrishnan, G.; Song, J.; Mou, C.; Bettinger, C. J.; Balakrishnan, G.; Song, J.; Mou, C.; Bettinger, C. J. Recent Progress in Materials Chemistry to Advance Flexible Bioelectronics in Medicine. *Adv. Mater.* **2022**, *34* (10), 2106787. https://doi.org/10.1002/ADMA.202106787.

(11) Zeglio, E.; Rutz, A. L.; Winkler, T. E.; Malliaras, G. G.; Herland, A.; Zeglio, E.; Winkler, T. E.; Herland, A.; Rutz, A. L.; Malliaras, G. G. Conjugated Polymers for Assessing and Controlling Biological Functions. *Adv. Mater.* **2019**, *31* (22), 1806712. https://doi.org/10.1002/ADMA.201806712.

(12) Inal, S.; Rivnay, J.; Suiu, A. O.; Malliaras, G. G.; McCulloch, I. Conjugated Polymers in Bioelectronics. *Acc. Chem. Res.* **2018**, *51* (6), 1368–1376. https://doi.org/10.1021/ACS.ACCOUNTS.7B00624.

(13) Zheng, Y.; Zhang, S.; Tok, J. B. H.; Bao, Z. Molecular Design of Stretchable Polymer Semiconductors: Current Progress and Future Directions. *J. Am. Chem. Soc.* **2022**, *144* (11), 4699–4715. https://doi.org/10.1021/JACS.2C00072.

(14) Zheng, Y.; Yu, Z.; Zhang, S.; Kong, X.; Michaels, W.; Wang, W.; Chen, G.; Liu, D.; Lai, J. C.; Prine, N.; Zhang, W.; Nikzad, S.; Cooper, C. B.; Zhong, D.; Mun, J.; Zhang, Z.; Kang, J.; Tok, J. B. H.; McCulloch, I.; Qin, J.; Gu, X.; Bao, Z. A Molecular Design Approach towards Elastic and Multifunctional Polymer Electronics. *Nat. Commun.* **2021**, *12* (1), 1–11. https://doi.org/10.1038/s41467-021-25719-9.

(15) Someya, T.; Bao, Z.; Malliaras, G. G. The Rise of Plastic Bioelectronics. *Nature* **2016**, *540* (7633), 379–385. https://doi.org/10.1038/nature21004.

(16) Won, S. M.; Cai, L.; Gutruf, P.; Rogers, J. A. Wireless and Battery-Free Technologies for Neuroengineering. *Nat. Biomed. Eng.* **2023**, *7*, 405–423. https://doi.org/10.1038/s41551-021-00683-3.

(17) Li, C.; Guo, C.; Fitzpatrick, V.; Ibrahim, A.; Zwierstra, M. J.; Hanna, P.; Lechtig, A.; Nazarian, A.; Lin, S. J.; Kaplan, D. L. Design of Biodegradable, Implantable Devices towards Clinical Translation. *Nat. Rev. Mater.* **2020**, *5*, 61–81. https://doi.org/10.1038/s41578-019-0150-z.

(18) Lin, A.; Uva, A.; Babi, J.; Tran, H. Materials Design for Resilience in the Biointegration of Electronics. *MRS Bull.* **2021**, *46* (9), 860–869. https://doi.org/10.1557/S43577-021-00174-5.

(19) Chiong, J. A.; Tran, H.; Lin, Y.; Zheng, Y.; Bao, Z.; Chiong, J. A.; Zheng, Y.; Tran, H.; Lin, Y.; Bao, Z. Integrating Emerging Polymer Chemistries for the Advancement of Recyclable, Biodegradable, and Biocompatible Electronics. *Adv. Sci.* **2021**,

8 (14), 2101233. https://doi.org/10.1002/ADVS.202101233.
(20) Uva, A.; Lin, A.; Babi, J.; Tran, H. Bioderived and Degradable Polymers for Transient Electronics. *J. Chem. Technol. Biotechnol.* **2022**, *97* (4), 801–809. https://doi.org/10.1002/JCTB.6790.
(21) Tropp, J.; Rivnay, J. Design of Biodegradable and Biocompatible Conjugated Polymers for Bioelectronics. *J. Mater. Chem. C* **2021**, *9* (39), 13543–13556. https://doi.org/10.1039/D1TC03600A.
(22) Nozaki, N.; Uva, A.; Matsumoto, H.; Tran, H.; Ashizawa, M. Thienoisoindigo-Based Recyclable Conjugated Polymers for Organic Electronics. *ChemRxiv* **2023**. https://doi.org/10.26434/chemrxiv-2023-rgm98.
(23) Bartlett, K. A.; Charland-Martin, A.; Lawton, J.; Tomlinson, A. L.; Collier, G. S. Azomethine-Containing Pyrrolo[3,2-b]Pyrrole Copolymers for Simple and Degradable Conjugated Polymers. *Macromol. Rapid Commun.* **2023**, 2300220. https://doi.org/10.1002/MARC.202300220.
(24) Lei, T.; Guan, M.; Liu, J.; Lin, H. C.; Pfattner, R.; Shaw, L.; McGuire, A. F.; Huang, T. C.; Shao, L.; Cheng, K. T.; Tok, J. B. H.; Bao, Z. Biocompatible and Totally Disintegrable Semiconducting Polymer for Ultrathin and Ultralightweight Transient Electronics. *Proc. Natl. Acad. Sci. U. S. A.* **2017**, *114* (20), 5107–5112. https://doi.org/10.1073/pnas.1701478114.
(25) Tran, H.; Feig, V. R.; Liu, K.; Wu, H. C.; Chen, R.; Xu, J.; Deisseroth, K.; Bao, Z. Stretchable and Fully Degradable Semiconductors for Transient Electronics. *ACS Cent. Sci.* **2019**, *5* (11), 1884–1891. https://doi.org/10.1021/ACSCENTSCI.9B00850.
(26) Bolduc, A.; Dufresne, S.; Skene, W. G. Chemical Doping of EDOT Azomethine Derivatives: Insight into the Oxidative and Hydrolytic Stability. *J. Mater. Chem.* **2012**, *22* (11), 5053–5064. https://doi.org/10.1039/C2JM14248A.
(27) Bolduc, A.; Dufresne, S.; Skene, W. G. EDOT-Containing Azomethine: An Easily Prepared Electrochromically Active Material with Tuneable Colours. *J. Mater. Chem.* **2010**, *20* (23), 4820–4826. https://doi.org/10.1039/B923821B.
(28) Bourgeaux, M.; Skene, W. G. Photophysics and Electrochemistry of Conjugated Oligothiophenes Prepared by Using Azomethine Connections. *J. Org. Chem.* **2007**, *72* (23), 8882–8892. https://doi.org/10.1021/JO701515J.
(29) Tran, H.; Nikzad, S.; Chiong, J. A.; Schuster, N. J.; Peña-Alcántara, A. E.; Feig, V. R.; Zheng, Y. Q.; Bao, Z. Modular Synthesis of Fully Degradable Imine-Based Semiconducting p-Type and n-Type Polymers. *Chem. Mater.* **2021**, *33* (18), 7465–7474. https://doi.org/10.1021/ACS.CHEMMATER.1C02258.
(30) Chiong, J. A.; Zheng, Y.; Zhang, S.; Ma, G.; Wu, Y.; Ngaruka, G.; Lin, Y.; Gu, X.; Bao, Z. Impact of Molecular Design on Degradation Lifetimes of Degradable Imine-Based Semiconducting Polymers. *J. Am. Chem. Soc.* **2022**, *144* (8), 3717–3726. https://doi.org/10.1021/JACS.1C12845.
(31) Uva, A.; Lin, A.; Tran, H. Biobased, Degradable, and Conjugated Poly(Azomethine)S. *J. Am. Chem. Soc.* **2023**, *145* (6), 3606–3614. https://doi.org/10.1021/JACS.2C12668.
(32) Gobalasingham, N. S.; Thompson, B. C. Direct Arylation Polymerization: A Guide to Optimal Conditions for Effective Conjugated Polymers. *Prog. Polym. Sci.* **2018**, *83*, 135–201. https://doi.org/10.1016/J.PROGPOLYMSCI.2018.06.002.
(33) Suraru, S. L.; Lee, J. A.; Luscombe, C. K. C-H Arylation in the Synthesis of π-Conjugated Polymers. *ACS Macro Lett.* **2016**, *5* (6), 724–729. https://doi.org/10.1021/ACSMACROLETT.6B00279.
(34) Pouliot, J. R.; Grenier, F.; Blaskovits, J. T.; Beaupré, S.; Leclerc, M. Direct (Hetero)Arylation Polymerization: Simplicity for Conjugated Polymer Synthesis. *Chem. Rev.* **2016**, *116* (22), 14225–14274. https://doi.org/10.1021/ACS.CHEMREV.6B00498.
(35) Zheng, Y.; Wang, G. J. N.; Kang, J.; Nikolka, M.; Wu, H. C.; Tran, H.; Zhang, S.; Yan, H.; Chen, H.; Yuen, P. Y.; Mun, J.; Dauskardt, R. H.; McCulloch, I.; Tok, J. B. H.; Gu, X.; Bao, Z. An Intrinsically Stretchable High-Performance Polymer Semiconductor with Low Crystallinity. *Adv. Funct. Mater.* **2019**, *29* (46), 1905340. https://doi.org/10.1002/ADFM.201905340.
(36) Bura, T.; Beaupré, S.; Légaré, M. A.; Quinn, J.; Rochette, E.; Blaskovits, J. T.; Fontaine, F. G.; Pron, A.; Li, Y.; Leclerc, M. Direct Heteroarylation Polymerization: Guidelines for Defect-Free Conjugated Polymers. *Chem. Sci.* **2017**, *8* (5), 3913–3925. https://doi.org/10.1039/C7SC00589J.
(37) Li, Y.; Tatum, W. K.; Onorato, J. W.; Zhang, Y.; Luscombe, C. K. Low Elastic Modulus and High Charge Mobility of Low-Crystallinity Indacenodithiophene-Based Semiconducting Polymers for Potential Applications in Stretchable Electronics. *Macromolecules.* **2018**, *51* (16), 6352–6358. https://doi.org/10.1021/ACS.MACROMOL.8B00898.
(38) Wadsworth, A.; Chen, H.; Thorley, K. J.; Cendra, C.; Nikolka, M.; Bristow, H.; Moser, M.; Salleo, A.; Anthopoulos, T. D.; Sirringhaus, H.; McCulloch, I. Modification of Indacenodithiophene-Based Polymers and Its Impact on Charge Carrier Mobility in Organic Thin-Film Transistors. *J. Am. Chem. Soc.* **2020**, *142* (2), 652–664. https://doi.org/10.1021/JACS.9B09374.
(39) Cendra, C.; Balhorn, L.; Zhang, W.; O'Hara, K.; Bruening, K.; Tassone, C. J.; Steinrück, H. G.; Liang, M.; Toney, M. F.; McCulloch, I.; Chabinyc, M. L.; Salleo, A.; Takacs, C. J. Unraveling the Unconventional Order of a High-Mobility Indacenodithiophene-Benzothiadiazole Copolymer. *ACS Macro Lett.* **2021**, *10* (10), 1306–1314. https://doi.org/10.1021/ACSMACROLETT.1C00547.
(40) Zhang, X.; Bronstein, H.; Kronemeijer, A. J.; Smith, J.; Kim, Y.; Kline, R. J.; Richter, L. J.; Anthopoulos, T. D.; Sirringhaus, H.; Song, K.; Heeney, M.; Zhang, W.; McCulloch, I.; Delongchamp, D. M. Molecular Origin of High Field-Effect Mobility in an Indacenodithiophene–Benzothiadiazole Copolymer. *Nat. Commun.* **2013**, *4*, 2238. https://doi.org/10.1038/ncomms3238.
(41) Sommerville, P. J. W.; Balzer, A. H.; Lecroy, G.; Guio, L.; Wang, Y.; Onorato, J. W.; Kukhta, N. A.; Gu, X.; Salleo, A.; Stingelin, N.; Luscombe, C. K. Influence of Side Chain Interdigitation on Strain and Charge Mobility of Planar Indacenodithiophene Copolymers. *ACS Polym. Au.* **2023**, *3* (1), 59–69. https://doi.org/10.1021/ACSPOLYMERSAU.2C00034.
(42) Ponder, J. F.; Chen, H.; Luci, A. M. T.; Moro, S.; Turano, M.; Hobson, A. L.; Collier, G. S.; Perdigão, L. M. A.; Moser, M.; Zhang, W.; Costantini, G.; Reynolds, J. R.; McCulloch, I. Low-Defect, High Molecular Weight Indacenodithiophene (IDT) Polymers Via a C-H Activation: Evaluation of a Simpler and Greener Approach to Organic Electronic Materials. *ACS Mater. Lett.* **2021**, *3* (10), 1503–1512. https://doi.org/10.1021/ACSMATERIALSLETT.1C00478.
(43) Adamczak, D.; Passarella, B.; Komber, H.; Becker-Koch, D.; Dolynchuk, O.; Schmidt, S. B.; Vaynzof, Y.; Caironi, M.; Sommer, M. Temperature-Dependent Morphology-Electron Mobility Correlations of Naphthalene Diimide-Indacenodithiophene Copolymers Prepared via Direct Arylation Polymerization. *Mater. Adv.* **2021**, *2* (24), 7881–7890. https://doi.org/10.1039/D1MA00633A.
(44) Gao, Y.; Zhang, X.; Tian, H.; Zhang, J.; Yan, D.; Geng, Y.; Wang Gao, F. Y.; Zhang, X.; Tian, H.; Zhang, J.; Yan, D.; Geng, Y.; Wang, F.; Gao, Y. High Mobility Ambipolar Diketopyrrolopyrrole-Based Conjugated Polymer Synthesized Via Direct Arylation Polycondensation. *Adv. Mater.* **2015**, *27* (42), 6753–6759. https://doi.org/10.1002/ADMA.201502896.
(45) Pankow, R. M.; Thompson, B. C. The Development of Conjugated Polymers as the Cornerstone of Organic Electronics. *Polymer* **2020**, *207*, 122874. https://doi.org/10.1016/J.POLYMER.2020.122874.
(46) Iizuka, E.; Wakioka, M.; Ozawa, F. Mixed-Ligand Approach to Palladium-Catalyzed Direct Arylation Polymerization: Effective Prevention of Structural Defects Using Diamines. *Macromolecules.* **2016**, *49* (9), 3310–3317. https://doi.org/10.1021/ACS.MACROMOL.6B00441.
(47) Wakioka, M.; Takahashi, R.; Ichihara, N.; Ozawa, F. Mixed-Ligand Approach to Palladium-Catalyzed Direct Arylation Polymerization: Highly Selective Synthesis of π-Conjugated Polymers with Diketopyrrolopyrrole Units. *Macromolecules.* **2017**, *50* (3), 927–934.

https://doi.org/10.1021/ACS.MACROMOL.6B02679.
(48) Wakioka, M.; Torii, N.; Saito, M.; Osaka, I.; Ozawa, F. Donor-Acceptor Polymers Containing 4,8-Dithienylbenzo[1,2- b:4,5-B′]Dithiophene via Highly Selective Direct Arylation Polymerization. *ACS Appl. Polym. Mater.* **2021**, *3* (2), 830–836. https://doi.org/10.1021/ACSAPM.0C01163.
(49) Matsidik, R.; Komber, H.; Luzio, A.; Caironi, M.; Sommer, M. Defect-Free Naphthalene Diimide Bithiophene Copolymers with Controlled Molar Mass and High Performance via Direct Arylation Polycondensation. *J. Am. Chem. Soc.* **2015**, *137* (20), 6705–6711. https://doi.org/10.1021/JACS.5B03355.
(50) Chávez, P.; Bulut, I.; Fall, S.; Ibraikulov, O. A.; Chochos, C. L.; Bartringer, J.; Heiser, T.; Lévêque, P.; Leclerc, N. An Electron-Transporting Thiazole-Based Polymer Synthesized Through Direct (Hetero)Arylation Polymerization. *Molecules* **2018**, *23* (6), 1270. https://doi.org/10.3390/MOLECULES23061270.
(51) Lu, W.; Kuwabara, J.; Kanbara, T. Polycondensation of Dibromofluorene Analogues with Tetrafluorobenzene via Direct Arylation. *Macromolecules.* **2011**, *44* (6), 1252–1255. https://doi.org/10.1021/MA1028517.
(52) Sun, H. Y.; Gorelsky, S. I.; Stuart, D. R.; Campeau, L. C.; Fagnou, K. Mechanistic Analysis of Azine N-Oxide Direct Arylation: Evidence for a Critical Role of Acetate in the Pd(OAc)2 Precatalyst. *J. Org. Chem.* **2010**, *75* (23), 8180–8189. https://doi.org/10.1021/JO101821R.
(53) Wang, X.; Wang, M. Synthesis of Donor–Acceptor Conjugated Polymers Based on Benzo[1,2- B :4,5- b ′]Dithiophene and 2,1,3-Benzothiadiazole via Direct Arylation Polycondensation: Towards Efficient C–H Activation in Nonpolar Solvents. *Polym. Chem.* **2014**, *5* (19), 5784–5792. https://doi.org/10.1039/C4PY00565A.
(54) Park, H.; Kim, Y.; Kim, D.; Lee, S.; Kim, F. S.; Kim, B. J.; Park, H.; Kim, Y.; Lee, S.; Kim, B. J.; Kim, D.; Kim, F. S. Disintegrable N-Type Electroactive Terpolymers for High-Performance, Transient Organic Electronics. *Adv. Funct. Mater.* **2022**, *32* (2), 2106977. https://doi.org/10.1002/ADFM.202106977.
(55) Barik, S.; Bletzacker, T.; Skene, W. G. π-Conjugated Fluorescent Azomethine Copolymers: Opto-Electronic, Halochromic, and Doping Properties. *Macromolecules.* **2012**, *45* (3), 1165–1173. https://doi.org/10.1021/MA2024304.
(56) Nitschke, P.; Jarząbek, B.; Bejan, A. E.; Damaceanu, M. D. Effect of Protonation on Optical and Electrochemical Properties of Thiophene-Phenylene-Based Schiff Bases with Alkoxy Side Groups. *J. Phys. Chem. B* **2021**, *125* (30), 8588–8600. https://doi.org/10.1021/ACS.JPCB.1C05390.
(57) Bejan, A. E.; Damaceanu, M. D. New Heterocyclic Conjugated Azomethines Containing Triphenylamine Units with Optical and Electrochemical Responses towards the Acid Environment. *Synth. Met.* **2020**, *268*, 116498. https://doi.org/10.1016/J.SYNTHMET.2020.116498.
(58) Casado, J.; Ortiz, R. P.; Navarrete, J. T. L. Quinoidal Oligothiophenes: New Properties behind an Unconventional Electronic Structure. *Chem. Soc. Rev.* **2012**, *41* (17), 5672–5686. https://doi.org/10.1039/C2CS35079C.
(59) Paterson, A. F.; Singh, S.; Fallon, K. J.; Hodsden, T.; Han, Y.; Schroeder, B. C.; Bronstein, H.; Heeney, M.; McCulloch, I.; Anthopoulos, T. D.; Paterson, A. F.; McCulloch, I.; Anthopoulos, T. D.; Singh, S.; Schroeder, B. C.; Fallon, K. J.; Bronstein, H.; Hodsden, T.; Han, Y.; Heeney, M. Recent Progress in High-Mobility Organic Transistors: A Reality Check. *Adv. Mater.* **2018**, *30* (36), 1801079. https://doi.org/10.1002/ADMA.201801079.
(60) Zhang, C.; Zhu, X.; Zhang, C.; Zhu, X. N-Type Quinoidal Oligothiophene-Based Semiconductors for Thin-Film Transistors and Thermoelectrics. *Adv. Funct. Mater.* **2020**, *30* (31), 2000765. https://doi.org/10.1002/ADFM.202000765.
(61) Casado, J.; Tobe, Y.; Kubo, T.; Es, C. Para-Quinodimethanes: A Unified Review of the Quinoidal-Versus-Aromatic Competition and Its Implications. *Top. Curr. Chem. 2017 3754* **2017**, *375* (4), 1–40. https://doi.org/10.1007/S41061-017-0163-2.
(62) Wałęsa-Chorab, M.; Tremblay, M. H.; Skene, W. G. Hydrogen-Bond and Supramolecular-Contact Mediated Fluorescence Enhancement of Electrochromic Azomethines. *Chem. – A Eur. J.* **2016**, *22* (32), 11382–11393. https://doi.org/10.1002/CHEM.201600859.
(63) Barik, S.; Skene, W. G. A Fluorescent All-Fluorene Polyazomethine—towards Soluble Conjugated Polymers Exhibiting High Fluorescence and Electrochromic Properties. *Polym. Chem.* **2011**, *2* (5), 1091–1097. https://doi.org/10.1039/C0PY00394H.
(64) Hu, B.; Zhu, X.; Chen, X.; Pan, L.; Peng, S.; Wu, Y.; Shang, J.; Liu, G.; Yan, Q.; Li, R. W. A Multilevel Memory Based on Proton-Doped Polyazomethine with an Excellent Uniformity in Resistive Switching. *J. Am. Chem. Soc.* **2012**, *134* (42), 17408–17411. https://doi.org/10.1021/JA307933T.
(65) Kato, T.; Gon, M.; Tanaka, K.; Chujo, Y. Modulation of Stimuli-Responsiveness toward Acid Vapor between Real-Time and Write-Erase Responses Based on Conjugated Polymers Containing Azobenzene and Schiff Base Moieties. *J. Polym. Sci.* **2021**, *59* (14), 1596–1602. https://doi.org/10.1002/POL.20210329.

For Table of Contents Only

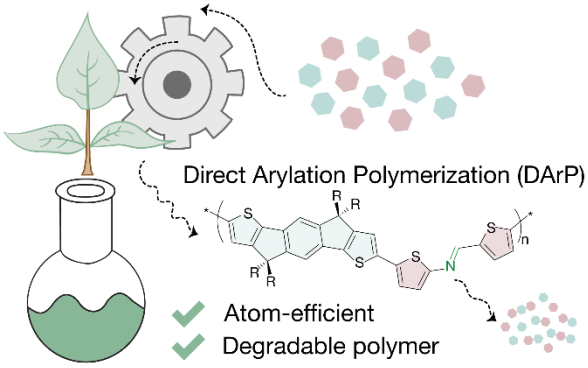

Synopsis: This work represents the synthesis of degradable imine-based conjugated polymers by direct arylation polymerization, a greener and more atom-efficient method than traditional polymerization methods.